CrossMark

Nanocomposite SAC Solders: The Effect of Adding Ni and Ni-Sn Nanoparticles on Morphology and Mechanical Properties of Sn-3.0Ag-0.5Cu Solders

A. YAKYMOVYCH [1,2,5] P. ŠVEC SR.,[3] L. OROVCIK,[4] O. BAJANA,[4] and H. IPSER[1]

1.—Department of Inorganic Chemistry – Functional Materials, Faculty of Chemistry, University of Vienna, Althanstr. 14, Währinger Str. 42, 1090 Vienna, Austria. 2.—Department of Metal Physics, Ivan Franko National University, Kyrylo and Mephodiy Str. 8, Lviv 79005, Ukraine. 3.—Department of Metal Physics, Institute of Physics, Slovak Academy of Sciences, Dubravska Cesta 9, 84511 Bratislava, Slovakia. 4.—Institute of Materials and Machine Mechanics, Slovak Academy of Sciences, Dubravska Cesta 9, 84511 Bratislava, Slovakia. 5.—e-mail: andriy.yakymovych@univie.ac.at

This study investigates the effect of minor additions of Ni, Ni_3Sn or Ni_3Sn_2 nanoparticles on the microstructure and mechanical properties of Cu/solder/Cu joints. The nanocomposite Sn-3.0Ag-0.5Cu (SAC305) solders with 0.5, 1.0 and 2.0 wt.% metallic nanoparticles were prepared through a paste mixing method. The employed Ni and Ni-Sn nanoparticles were produced via a chemical reduction method. The microstructure of as-solidified Cu/solder/Cu joints was studied by x-ray diffraction and scanning electron microscopy. The results showed that additions of Ni and Ni-Sn nanoparticles to the SAC305 solder paste lead initially to a decrease in the average thickness of the intermetallic compound layer in the interface between solder and substrate, while further additions up to 2.0 wt.% did not induce any significant changes. In addition, shear strength and microhardness tests were performed to investigate the relationship between microstructure and mechanical properties of the investigated solder joints. The results indicated an increase in both of these properties which was most significant for the solder joints using SAC305 with 0.5 wt.% Ni or Ni-Sn nanoparticles.

Key words: Sn3.0Ag0.5Cu, Ni and Ni-Sn nanoparticles, microstructure, shear strength, microhardness

INTRODUCTION

So far, the development of commercial solder joints has focused on using lead-free Sn-based solders reinforced with different kinds of nanoparticles.[1–4] All these studies showed a profound impact of various ceramic and metal nanoparticles (NPs) on the microstructure and mechanical properties of Sn-Ag-Cu (SAC) solders and the corresponding solder joints. For instance, Refs. 5 and 6 showed a reinforced microstructure with relatively small intermetallic compound (IMC) grains homogeneously distributed in the Sn matrix. The noticeable changes in the morphology and thickness of the interfacial IMC layer between solder and substrate for nanocomposite solder joints were shown in Refs. 7 and 8. Furthermore, the additions of NPs to the SAC solders lead to an enhancement of the shear strength, microhardness, wettability and of other properties.[9–11]

In all these studies, it was shown that the additions of different kinds of NPs to the SAC solders lead, in principle, to similar effects. However, the behavior of the employed ceramic nanoinclusions in the Sn-based matrix is fundamentally

different from that of metallic NPs: metal NPs are dissolved during the soldering process and act through an alloying effect while ceramic NPs act as nuclei for heterogeneous nucleation. The reduction of the average size of the IMC layer at the interface solder/substrate using nanocomposite SAC solders with ceramic nanoinclusions is explained by the formation of a diffusion barrier layer between the solder and the substrate to retard the rapid interfacial reaction. A similar reduction of the IMC layer, compared to unreinforced SAC solder joints, has been described for nanocomposite SAC solders with metallic NPs, such as Co, Ni, etc., where part of the added metal is apparently dissolved in the compound Cu_6Sn_5.[7,12]

Several methods have been developed for the introduction of NPs into the SAC solders. For instance, a paste and flux mixing method was applied to prepare solders in paste form or as nanocomposite flux-solder mixture, respectively.[7,8,13,14] A conventional planar flow casting[9,15] as well as a roll bonding method[16] have been used to fabricate nanocomposite solder ribbons. The mixing methods are the most popular ones due to the relatively simple experimental procedure; however, during the reflow process the NPs tend to move with the flux, and it is very difficult to estimate the amount of nanoinclusions actually remaining in the solder.

Among various types of nanoinclusions in the SAC solders, Ni has attracted great interest due to significant beneficial effects, such as improved microhardness,[6] wettability[7] and reliability of the solder joints.[14] For instance, the SAC solders and solder joints with Ni as alloying element[17,18] or as addition in form of micro- or NPs were intensively investigated in Refs. 6, 7, 14, and 19–21.

In this work, we report the changes of microstructure and mechanical properties (shear strength and microhardness) of Cu/SAC305/Cu solder joints caused by minor additions of Ni and intermetallic Ni_3Sn and Ni_3Sn_2 NPs. The nanocomposite solders with 0.5, 1.0 and 2.0 wt.% nanoinclusions were prepared by the paste mixing method. The Ni and Ni-Sn nanoinclusions modified the morphology of the SAC305 solder joints and had a noticeable influence on the average thickness of the intermetallic layer at the interface between solder and substrate.

EXPERIMENTAL PROCEDURES

The Sn-3.0Ag-0.5Cu (SAC305) solder paste provided by Kester (USA) and home-made nanopowders of Ni, Ni_3Sn and N_3Sn_2 were mixed together in a mortar within a glovebox for at least 30 min to form nanocomposite solders at a nominal percentage of 0.5, 1.0 and 2.0 wt.% (related to the mass of the solder in the paste). It was found that 30 min should be enough to achieve a homogeneous distribution of NPs in the solder paste.[6,7]

The Ni and Ni-Sn NPs were produced via a chemical reduction method employing hydrazine hydrate ($N_2H_4 \cdot H_2O$; Sigma-Aldrich) and polyvinylpyrrolidone (PVP; Alfa-Aesar) as reducing and surfactant agents, respectively. Nickel chloride ($NiCl_2$; Loba-Chemie, Austria) and tin(II)-2-ethylhexanoate ($C_{16}H_{30}O_4Sn$; Alfa-Aesar) were dissolved in diethylene glycol (DEG; Alfa-Aesar) as the metal precursors. The average size of the produced Ni and Ni-Sn NPs was about 100 nm (Fig. 1). The experimental procedure was described in detail elsewhere.[22]

The solder joints were produced using 3-mm-thick Cu disks with diameters of 10 mm and 15 mm as substrates. Before laying down the nanocomposite solder paste, the Cu plates were ground and polished with 1-μm and 0.3-μm Al_2O_3 powders, cleaned with ethanol and immerged into a 10 vol.% sulfuric acid solution (10 vol.% H_2SO_4 + 90 vol.% C_2H_5OH) for 2 min to remove the oxide layer on the surface. The Cu/solder/Cu holders were placed into an electric resistance furnace, and the joints were prepared in air atmosphere by heating at 523 K for 300 s (Fig. 2). After the reflow, the solder joints were cleaned to remove any flux residue.

One part of the reflowed samples was cross-sectioned and polished with 1-μm and 0.3-μm Al_2O_3 powders for microstructure analysis. The microstructure of the joints was studied by scanning electron microscopy (SEM; JEOL JSM 6610 and JEOL JSM-7600F equipped with an energy dispersive x-ray (EDX) analyzer [Oxford Instruments (OI), X-max 50 mm^2]. For surface observation, the COMPO and the SEI mode were used. The average thickness of the IMC layer at the interface between the solder and the substrate was calculated using the Digimizer software, freely available in the Internet.[23] The following equation was used to calculate the average thickness, x:

$$x = S/L \tag{1}$$

where L is the length, and S is the integral contour area of the intermetallic layer at the interface.

Another part of the produced samples was used for measurements of mechanical properties. The shear strength studies were performed by the push-off method (Zwick/Roell Z 100), employing a shearing speed of 1×10^{-3} m min^{-1}. The microhardness was measured using a Microhardness Tester (FM-100, Future-Tech Corp.). The square-based pyramidal diamond was pressed using a force of 0.05 N for a loading time of 10 s; at least eight areas across each joint were tested in our measurements to obtain an average value.

RESULTS AND DISCUSSION

Microstructure Analysis

The effect of the addition of the metallic NPs on the growth of IMC particles in the bulk solder and
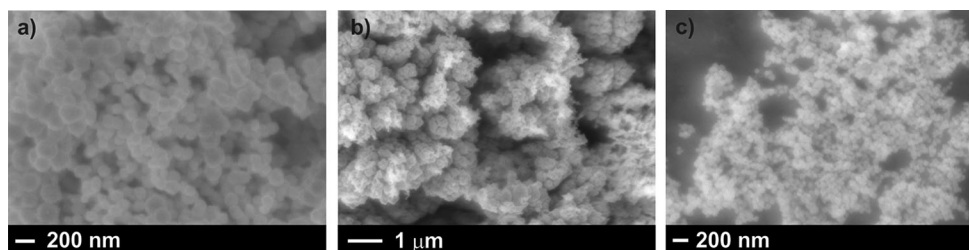
Nanocomposite SAC Solders: The Effect of Adding Ni and Ni-Sn Nanoparticles on Morphology
and Mechanical Properties of Sn-3.0Ag-0.5Cu Solders

119

Fig. 1. SEM micrographs of Ni (a), Ni_3Sn (b) and Ni_3Sn_2 (c) nanoparticles.
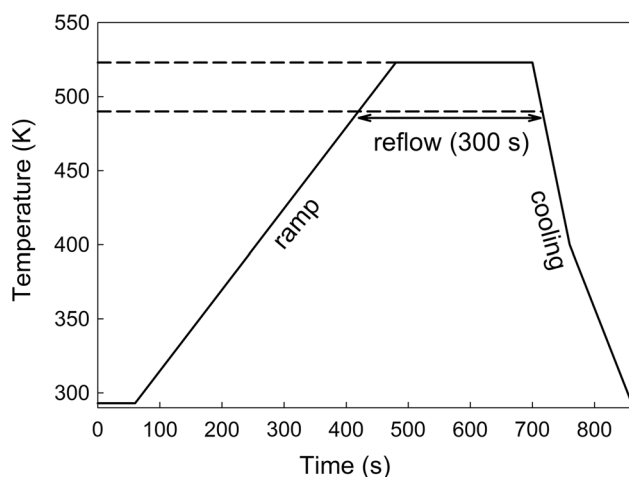

Fig. 2. Reflow temperature profile of solder/Cu joint.

at the interface of solder/Cu was investigated based on SEM of the prepared solder joints. It could be shown that the initial addition of pure Ni lead to a reinforcement of the microstructure of the bulk solder, i.e. the IMC grains were much smaller in the reinforced solder matrix as compared to the unreinforced sample (Figs. 3a and b). The same tendency was determined for solder joints with 1.0 and 2.0 wt.% Ni (Figs. 3c and d).

Furthermore, the addition of Ni NPs to the SAC305 solder joints lead to changes in the morphology of the interfacial IMC layer from the scallop type layer, typical for SAC solder joints (Fig. 3a), to a more planar-type shape (Figs. 3b–d). Similar changes were indicated for solder joints with nano Ni_3Sn_2 and nano Ni_3Sn additions. The same effect, i.e. a transformation of the IMC layer to a more planar shape with additions of nano Ni, was already observed in Refs. 7 and 14.

In view of this fact, we performed elemental mapping of the IMCs in the bulk solder and at the interface layer of the investigated solder joints. Similar to our previous studies dealing with nanocomposite SAC solder joints with metal and ceramic nanoadditions,[8,9] a Cu_6Sn_5/Cu_3Sn double layer was observed at the solder/Cu interface. It was found that Ni atoms were incorporated into the Cu_6Sn_5 crystals, both in the bulk solder and in the interfacial layer, while no regions with either pure

Ni or Ni-Sn IMCs could be seen in the joints. As an example, Fig. 4 presents the cross-sectional microstructure of solder/Cu solder joints without (a) and with 1.0 wt.% Ni (b), Ni_3Sn (c) and Ni_3Sn_2 (d) nanoinclusions, respectively. This phenomenon can be explained by the assumption that Ni and Ni-Sn particles were completely dissolved during the ramp and the reflow and $(Ni,Cu)_6Sn_5$ crystals were formed during cooling. At the same time, no traces of Ni were found in the Cu_3Sn and Ag_3Sn phases. A very similar observation was made in previous studies dealing with nanocomposite SAC solders with nano Ni.[7] It should also be noted that the relatively small light spheres in the presented micrographs (Fig. 3 and 4) correspond to Ag_3Sn grains homogeneously distributed in the bulk solder and dispersed on the surface of the interfacial IMC layer.

An EDX analysis of the $(Cu,Ni)_6Sn_5$ IMC, both in the bulk solder and in the interface layers, was performed for all investigated solder joints (see Table I), and this showed clearly that Ni atoms replace Cu in Cu_6Sn_5 according to its typical concentrations in the solder. The outer IMC layers at the interface solder/Cu and the IMCs in the solder matrix contained about 2 at.% Ni while the concentration of Ni in the IMC in the bulk solder near the interfacial layer reached about 17 at.%. These data are in agreement with results from Ref. 24 where a possible dissolution of 21.4 at.% Ni in Cu_6Sn_5 was shown. The higher amount of Ni in $(Cu,Ni)_6Sn_5$ grains located in the solder matrix close to the interface compared to its concentration in the interfacial IMC layer was explained in Ref. 6.

It should also be noted that the amount of dissolved Ni in $(Cu,Ni)_6Sn_5$ grains, both in the solder matrix and at the interface, was smaller when Ni-Sn intermetallic NPs were added to the SAC solder than for pure Ni NPs (Table I). Furthermore, according to the elemental mapping of solder/Cu joints with Ni_3Sn and Ni_3Sn_2 nanoinclusions, there are some areas in the interfacial IMC layer, which did not contain Ni at all. This observation is rather difficult to explain; however, it is clear that the total amount of Ni is less in the Ni-Sn NPs than in the pure Ni NPs. In addition, it is to be expected that the dissolution of the Ni-Sn NPs is slower due to the tin oxide/hydroxide shell that is to be expected on their surface.
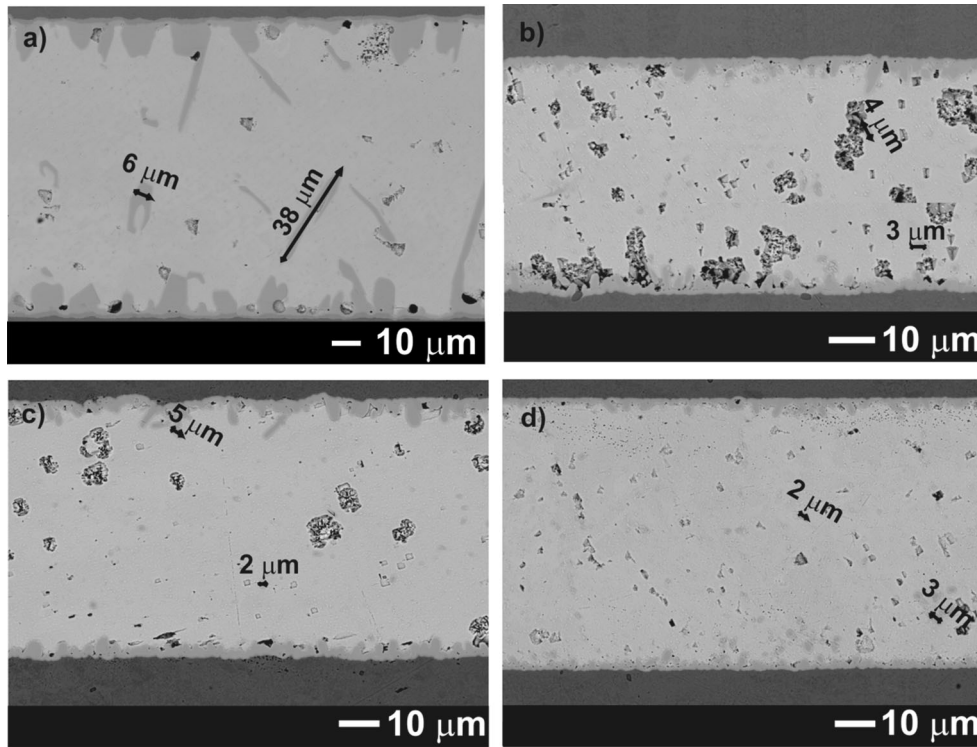
Fig. 3. SEM micrographs of as-solidified SAC305 (a) and SAC305-Ni solder joints with 0.5 (b), 1.0 (c) and 2.0 wt.% Ni (d).
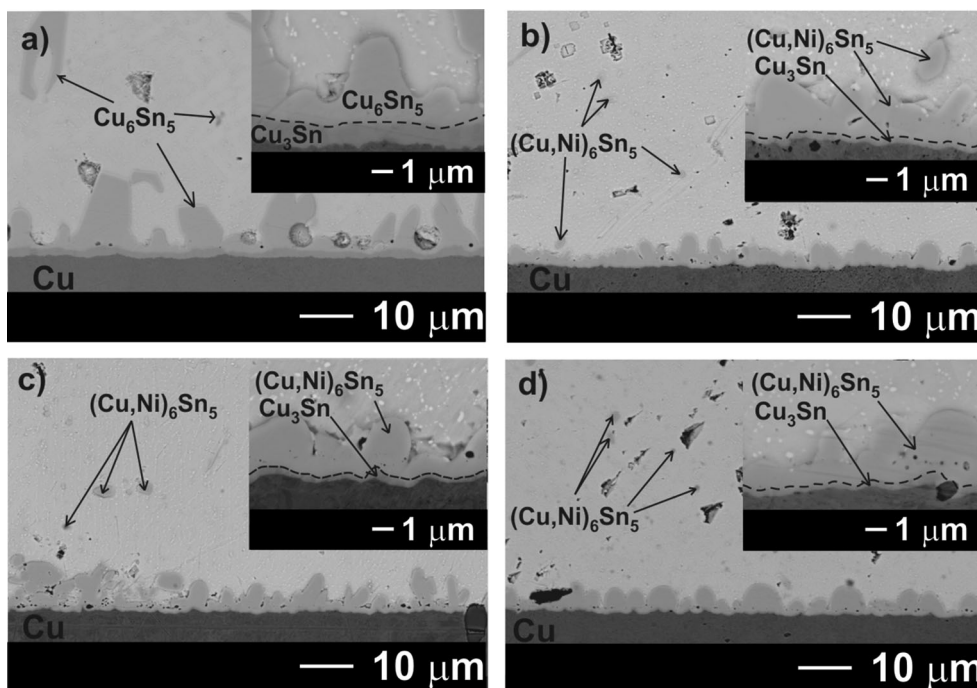

Fig. 4. SEM micrographs of as-solidified SAC305 (a) and SAC305 solder joints with 1.0 wt.% Ni (b), Ni_3Sn (c) and Ni_3Sn_2 (d).

Figure 5 shows the average thickness of the interfacial $(Cu,Ni)_6Sn_5 + Cu_3Sn$ layer between solder and Cu substrate. Initial additions of nanoinclusions lead to a decrease of the average thickness

while the most significant drop was obtained for the SAC305 solder joints with additions of 0.5 wt.% nano Ni. Further additions of nano Ni_3Sn up to 2.0 wt.% lead to an insignificant increase of the

Nanocomposite SAC Solders: The Effect of Adding Ni and Ni-Sn Nanoparticles on Morphology and Mechanical Properties of Sn-3.0Ag-0.5Cu Solders

121

Table I. EDX analysis of $(Cu,Ni)_6Sn_5$ grains in the bulk solder and in the interface layer

Solder alloy	Location of $(Cu,Ni)_6Sn_5$	Cu (in at.%)	Sn (in at.%)	Ni (in at.%)
SAC305 + Ni	Outer interfacial layer	54.9–57.2	41.3–43.9	1.1–1.7
(0.5, 1.0 and 2.0 wt.%)	Grains close to interfacial layer	37.7–40.2	44.9–54.0	5.0–17.4
	Solder matrix	55.1–56.4	42.6–42.1	1.1–2.4
		55.9–57.4	42.6–44.1	–
SAC305 + Ni$_3$Sn	Outer interfacial layer	53.4–58.7	39.8–45.4	0.8–2.2
(0.5, 1.0 and 2.0 wt.%)	Grains close to interfacial layer	41.2–56.8	41.9–52.0	1.3–6.8
	Solder matrix	55.8–56.9	41.9–42.3	1.1–1.9
		57.6–57.7	42.3–42.4	–
SAC305 + Ni$_3$Sn$_2$	Outer interfacial layer	52.1–58.9	40.0–46.8	0.1–1.4
(0.5, 1.0 and 2.0 wt.%)	Grains close to interfacial layer	44.4–59.0	40.5–50.6	0.5–4.0
	Solder matrix	55.3–56.4	42–43.1	0.2–1.6
		54.2–56.9	43.1–45.8	–
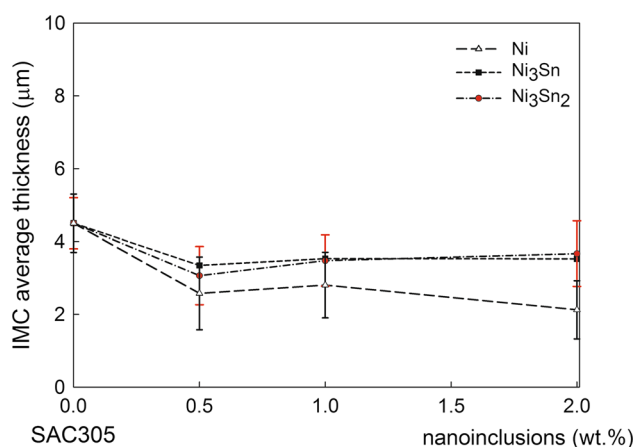
Fig. 5. The average thickness of the $(Cu,Ni)_6Sn_5$ + Cu$_3$Sn interface layer.

average thickness while the concentration dependence of the average thickness of the $(Cu,Ni)_6Sn_5$ + Cu$_3$Sn IMC layer at the solder/Cu interface shows a plateau for SAC305 solder joints with 0.5–2.0 wt.% nano Ni$_3$Sn$_2$. In contrast, the addition of 1.0 wt.% Ni to the SAC305 solder did not affect the average thickness of the interface IMCs layer while a further decrease was indicated for SAC305 solder joints with 2.0 wt.% Ni NPs. It should also be noted that a gradual transformation of the morphology of the interfacial layer from the typical scallop to a more planar type was indicated for the SAC305 solder joints with further additions of both Ni and Ni-Sn NPs. At the same time, the thickness of the thin Cu$_3$Sn layer in the interface zone was about 0.3 mm for all investigated solder joints. The present results are in a good agreement with literature data on the average thickness of the interfacial IMC layer for SAC305 + 0.5 wt.% nano Ni/Cu (2.42 μm; Ref. 6), but in some disagreement with literature data on SAC305 + 2.0 wt.% nano Ni/Cu (3.9 μm; Ref. 14). However, it should be pointed out that the solders for the joints investigated in Ref. 14 were prepared by the flux mixing method

where Ni NPs were concentrated in the flux between SAC solder ball and Cu substrate.

Based on the observations presented above, adding Ni in nanosized form to the SAC solders has several advantages compared to the addition of Ni in bulk form:

- Nanoadditions lead to a transition of the morphology of the interfacial IMC layer from a scallop to a more planar type, which should improve the joint strength, while needle-like microstructures were observed in SAC solder joints with bulk Ni additions which might deteriorate the mechanical properties;[17,25]
- In contrast to the bulk, nanoinclusions did not lead to the formation of large amounts of $(Cu,Ni)_6Sn_5$ grains near the solder/Cu interface as well as to a growth of the average thickness of the interfacial IMC layer.[18]

Mechanical Properties

The shear strength of the SAC solder joints with Ni and Ni-Sn nanoinclusions is presented in Fig. 6. A significant increase of the shear strength by initial additions of NPs to the SAC305 solder was found for all employed NPs while further additions did not show any considerable improvement of this mechanical property. It should be noted that the growth of brittle IMC layers at the interface solder/substrate affects the reliability of the solder joint considerably, in particular the shear strength. Therefore, the observed changes in the morphology and thickness of the interfacial layer should be directly connected with changes of the shear strength. In the present case, it was established that a noticeable decrease in the average thickness lead to an increase in the shear strength from 30 MPa up to 47 MPa.

The postulated reinforcement of the microstructure in the bulk solder should lead to an enhancement of the microhardness due to the pinning effect. The finely distributed small-sized particles (in the
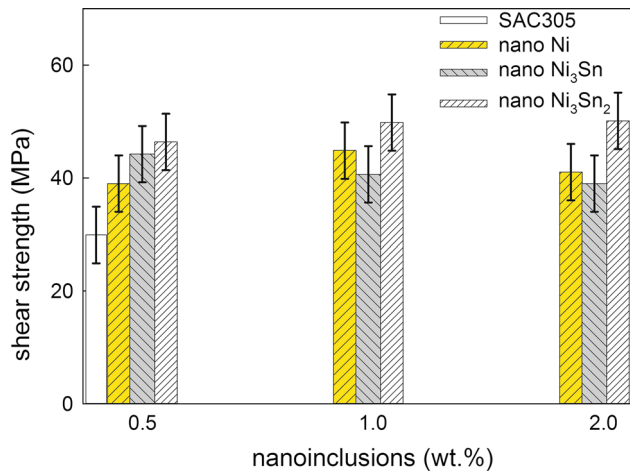
Fig. 6. The shear strength of the nanocomposite SAC305 solder joints as a function of the amount of Ni and Ni-Sn NPs.
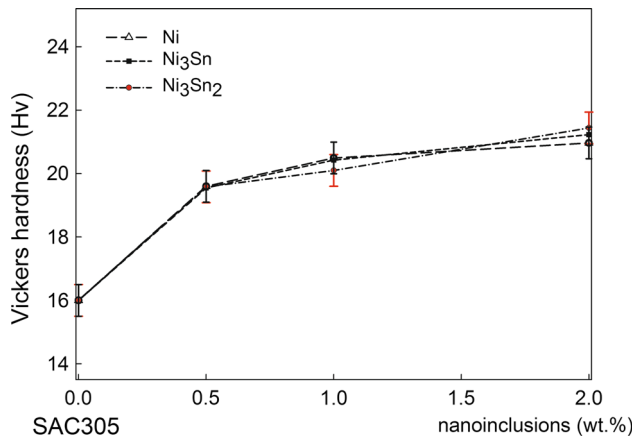

Fig. 7. The Vickers hardness of the nanocomposite SAC305 solder joints as a function of the amount of Ni and Ni-Sn nanoinclusions.

present case, Ag_3Sn and $Cu_6Sn_5/(Cu,Ni)_6Sn_5)$ improve the solder deformation resistance. According to the results presented in Fig. 7, the major effect of the addition of NPs was obtained for 0.5 wt.% of nanoinclusions. Further additions up to 2.0 wt.% improved the microhardness of the bulk SAC305 solder, however, less significantly compared to the initial addition. Such a significant increase in the microhardness for SAC305 solder (about 11%) with the addition of 0.5 wt.% nano Ni was also indicated by Gain and Chan.[6]

Finally, it should also be noted that we cannot estimate the exact amount of nano Ni which remained in the solder joints after the reflow process. The chemical analysis of the reinforced SAC solders with Ni NPs performed by Tay et al.[7] determined, for example, that for the addition of 2.0 wt.% NPs, only 0.29 wt.% Ni were left in the solder after the reflow.

CONCLUSIONS

Based on the present results, a complete dissolution of the employed nanoinclusions into the SAC305 solder during the reflow process is suggested. The major effects on the microstructure and mechanical properties of the SAC305 solder joints were caused by the initial additions of Ni, Ni_3Sn and Ni_3Sn_2 NPs (0.5 wt.%), while a further increase of the amount of nanoinclusions up to 2.0 wt.% did not lead to any significant further improvements. The average thickness of the interfacial IMC layer decreases significantly by the addition of nano Ni compared to the Ni-Sn nanoadditions. In contrast, the effect of the Ni, Ni_3Sn and Ni_3Sn_2 nanoadditions on the shear strength and the microhardness of the SAC305 solder joint is more or less the same.

ACKNOWLEDGEMENTS

OPEN ACCESS

REFERENCES

1. A.T. Tan, A.W. Tan, and F. Yusof, *Sci. Technol. Adv. Mat.* 16, 033505 (2015).
2. H.R. Kotadia, P.D. Howes, and S.H. Mannan, *Microelectron. Reliab.* 54, 1253 (2014).
3. L. Zhang and K.N. Tu, *Mat. Sci. Eng. R* 82, 1 (2014).
4. K. Subramanian, *Lead-Free Solders; Materials Reliability for Electronics* (Chichester: Wiley, 2012), p. 520.
5. L.C. Tsao, R.W. Wu, T.H. Cheng, K.H. Fan, and R.S. Chen, *Mater. Des.* 50, 774 (2013).
6. A.K. Gain and Y.C. Chan, *Intermetallics* 29, 48 (2012).
7. S.L. Tay, A.S.M.A. Haseeb, M.R. Johan, P.R. Munroe, and M.Z. Quadir, *Intermetallics* 33, 8 (2013).
8. A. Yakymovych, Y. Plevachuk, P. Svec, P. Svec, D. Janikovic, P. Sebo, N. Beronska, A. Roshanghias, and H. Ipser, *J. Electron. Mater.* 45, 6143 (2016).
9. A. Yakymovych, Y. Plevachuk, P. Svec, D. Janikovic, P. Sebo, N. Beronska, M. Nosko, L. Orovcik, A. Roshanghias, and H. Ipser, *J. Mater. Sci. Mater. Electron.* 28, 10965 (2017).
10. G. Chen, F.S. Wu, C.Q. Liu, V.V. Silberschmidt, and Y.C. Chan, *J. Alloys Compd.* 656, 500 (2016).
11. S. Chellvarajoo and M.Z. Abdullah, *Mater. Des.* 90, 499 (2016).
12. F. Gao, J.M. Qu, and T. Takemoto, *J. Electron. Mater.* 39, 426 (2010).
13. S.K. Ghosh, A.S.M.A. Haseeb, A. Afifi, *Electronics Packaging Technology Conference (EPTC 2013)* 21 (2013). doi: 10.1109/EPTC.2013.6745676.

Nanocomposite SAC Solders: The Effect of Adding Ni and Ni-Sn Nanoparticles on Morphology and Mechanical Properties of Sn-3.0Ag-0.5Cu Solders

123

14. M.N. Bashir, A.S.M.A. Haseeb, A.M.S. Rahman, M.A. Fazal, and C.R. Kao, *J. Mater. Sci.* 50, 6748 (2015).
15. K. Mehrabi, F. Khodabakhshi, E. Zareh, A. Shahbazkhan, and A. Simchi, *J. Alloys Compd.* 688, 143 (2016).
16. A. Roshanghias, A.H. Kokabi, Y. Miyashita, Y. Mutoh, M. Rezayat, and H.R. Madaah-Hosseini, *J. Mater. Sci. Mater. Electron.* 23, 1698 (2012).
17. Y.W. Wang, C.C. Chang, and C.R. Kao, *J. Alloys Compd.* 478, L1 (2009).
18. Y.W. Wang, C.R. Kao, *Electronic Materials and Packaging, 2008 (EMAP 2008)* 76 (2008). doi: 10.1109/EMAP.2008.4784233.
19. A. Yakymovych, Y. Plevachuk, V. Sklyarchuk, B. Sokoliuk, T. Galya, and H. Ipser, *J. Phase Equilib. Diffus.* 38, 217 (2017).
20. P. Yao, P. Liu, and J. Liu, *J. Alloys Compd.* 462, 73 (2008).
21. P. Liu, P. Yao, and J. Liu, *J. Alloys Compd.* 486, 474 (2009).
22. A. Yakymovych and H. Ipser, *Nanoscale Res. Lett.* 12, 142 (2017).
23. Med Calc Software BVBA, *Free Image Analysis Software* (2016). http://www.digimizer.com.
24. C.H. Wang, W.H. Lai, and S.W. Chen, *J. Electron. Mater.* 43, 195 (2014).
25. J.Y. Tsai, Y.C. Hu, C.M. Tsai, and C.R. Kao, *J. Electron. Mater.* 32, 1203 (2003).